Possible "Reentrant" Behavior in Magnetic Properties of TBA[Fe(tdas)$_2$] Complex

Kunio Awaga,*[1a] Tsunehisa Okuno,[1a] Yusei Maruyama,[1b] Akiko Kobayashi,[1c] Hayao Kobayashi,[1d] Stephen Schenk,[1e] and Allan E. Underhill*[1e]

Department of Pure and Applied Sciences, The University of Tokyo, Komaba, Meguro-ku, Tokyo 153, Japan, Institute for Molecular Science, Myodaiji, Okazaki 444, Japan, Department of Chemistry, Faculty of Science, The University of Tokyo, Hongo, Bunkyo-ku, Tokyo 113, Japan, Department of Chemistry, Faculty of Science, Toho University, Funabashi, Chiba 274, Japan, and Department of Chemistry and Institute of Molecular and Biomolecular Electronics, University of Wales, Bangor, Gwynedd LL57 UW, U.K.

Received March 2, 1993

Introduction

Extensive studies of metal complexes of multisulfur π-acceptor ligands have been carried out over the past ten years because of the unusual electrical, optical, and magnetic properties found for these compounds. Complexes of 1,2,5-thiadiazole-3,4-dithiolate (tdas) with Ni, Pd, Pt, Cu, or Fe have been reported.[2] We now report the first detailed investigation of the structure and unusual properties of a [Fe(tdas)$_2$] complex.

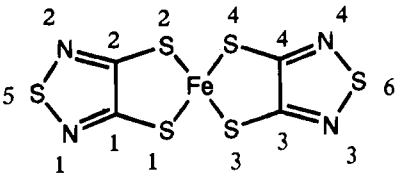

Results and Discussion

TBA[Fe(tdas)$_2$] (TBA = tetrabutylammonium) crystallizes into the triclinic $P\bar{1}$ space group. Figure 1 shows a view of the unit cell. The [Fe(tdas)$_2$]$^-$ ion is present as a centrosymmetric dimer, resulting in a distorted five-coordinate geometry around the iron. The average intramolecular Fe−S bond length is 2.245 Å, while the intermolecular Fe···S distance is 2.501 Å. Similarly, a five-coordinate pyramidal structure has been observed in some porphyrines,[3,4] the halobis(dithiocarbamates) Fe(X)(S$_2$CNR$_2$)$_2$ with X = Cl, Br, etc. and R = CH$_3$, C$_2$H$_5$, etc.,[5−10] and related compounds.

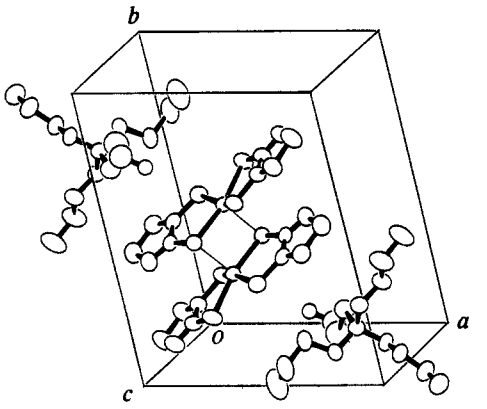

Figure 1. Crystal structure of TBA[Fe(tdas)$_2$].

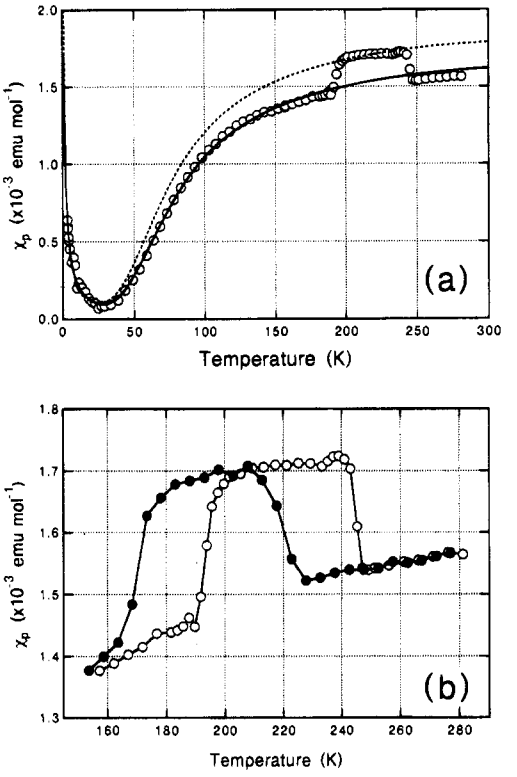

Figure 2. (a) Temperature dependence of the paramagnetic susceptibility, χ_p, of TBA[Fe(tdas)$_2$]. (b) Magnetic behavior above 150 K in an enlarged scale. The open and closed circles represent runs on heating and cooling, respectively.

The temperature dependence of the magnetic susceptibility was measured over the temperature range 3−280 K. The paramagnetic susceptibility, χ_p, was obtained by compensating for the Pascal diamagnetic susceptibility of -2.5×10^{-4} emu mol^{-1}. The open circles in Figure 2a show χ_p recorded with increasing temperature. The magnetic behaviors above 150 K are shown in Figure 2b in an enlarged scale. One can see Curie behavior below 30 K, which could be due to lattice defects. Above 30 K, χ_p starts to increase with increasing temperature, indicating that the intradimer magnetic interaction is antiferromagnetic. At 190 K, however, χ_p increases suddenly by *ca.* 10%, followed by a gradual increase up to 240 K. The second phase transition takes place at 240 K, and χ_p decreases rapidly by almost the same amount of the change at 190 K. In the high temperature phase above 240 K, χ_p continues to increase slightly. The closed circles in Figure 2b shows the change of χ_p which were recorded with decreasing temperature. The two magnetic transitions observed in the heating process also appear

(1) (a) Department of Pure and Applied Sciences, The University of Tokyo. (b) Institute for Molecular Science. (c) Department of Chemistry, The University of Tokyo. (d) Toho University. (e) University of Wales.
(2) Hawkins, I.; Underhill, A. E. *J. Chem. Soc., Chem. Commun.* **1990**, 1593.
(3) Perutz, M. F. *Nature* **1970**, *228*, 726 and references cited therein.
(4) Browett, W. R.; Fucaloro, A. F.; Morgan, T. V.; Stephens, P. J. *J. Am. Chem. Soc.* **1983**, *105*, 1868.
(5) Martin, R. L.; White, A. H. *Inorg. Chem.* **1967**, *6*, 712. Hoskins, B. F.; White, A. H. *J. Chem. Soc. A* **1970**, 1668.
(6) Hoskins, B. F.; White, A. H. *J. Chem. Soc. D* **1972**, 1369.
(7) Wickman, H. H. *J. Chem. Phys.* **1972**, *56*, 976.
(8) Chapps, G. E.; McCann, S. W.; Wickman, H. H.; Sherwood, R. C. *J. Chem. Phys.* **1974**, *60*, 990.
(9) DeFotis, G. C.; Palacio, F.; Carlin, R. L. *Phys. Rev. B* **1979**, *20*, 2945.
(10) DeFotis, G. C.; Cowen, J. A. *J. Chem. Phys.* **1980**, *73*, 2120.

0020-1669/94/1333-5598$04.50/0

on cooling the sample, making two large hysteresis loops which have the same width of *ca.* 20 K. The observations described above are indicative of first-order phase transitions.

The $S = {}^3/_2$ is likely to be the spin state in TBA[Fe(tdas)$_2$]: in an elongated square-pyramidal coordination the $d_{x^2-y^2}$ orbital is strongly σ-antibonding in contrast to d_{z^2}, leaving this state empty and indicating a redistribution of the five d-electrons according to $S = {}^3/_2$. In fact, Fe(X)(S$_2$CNR$_2$)$_2$ system[5-10] in which the Fe^{3+} ion has a similar coordination environment to that in TBA[Fe(tdas)$_2$], has aroused interest due to the unusual ground state with $S = {}^3/_2$. There is little difference in the Fe−S bond lengths of the distorted square planar arrangement of S atoms between the two systems. The axial intermolecular Fe···S distance in TBA[Fe(tdas)$_2$] is longer by *ca.* 0.25 Å than the corresponding Fe···X$^-$ distance in Fe(X)(S$_2$CNR$_2$)$_2$, but this could be compensated by the fact that the ligand field made by sulfur atoms is generally speaking, stronger than that made by halogen ions. Therefore, the Fe atoms in TBA[Fe(tdas)$_2$] and Fe(X)(S$_2$CNR$_2$)$_2$ are considered to be in a similar ligand field. In the following analysis, we will assume a $S = {}^3/_2$ spin state.

According to the crystal structure, we interpret the magnetic data in terms of the $S = {}^3/_2$ dimer model, using

$$\chi_p = \frac{N_A g^2 \mu_B{}^2}{k_B T} \frac{e^{-2J/k_BT} + 5e^{-2J/k_BT} + 14e^{-2J/k_BT}}{1 + 3e^{-2J/k_BT} + 5e^{-2J/k_BT} + 7e^{-2J/k_BT}} + \frac{C}{T} \quad (1)$$

where N_A is the Avogadro constant, g is the g factor, μ_B is the Bohr magneton, k_B is the Boltzmann constant, and J is the coupling constant. The second term is for fitting the Curie behavior below 30 K. The solid curve in Figure 2a shows the theoretical best fit obtained with the data below 180 K, whose parameters are $J/k_B = 118$ K, $g = 1.88$, and the Curie constant of $C = 1.4 \times 10^{-3}$ emu K mol^{-1}. The observed g factor is reasonable for Fe^{3+} within experimental error. It is notable that the theoretical curve not only fits well the data below 180 K but also explains the magnetic behavior above 240 K. This strongly suggests that the observed temperature dependence of χ_p can be understood as a reentrant behavior: the low temperature phase below 182 K (midpoint in the hysteresis loop) and the high temperature phase above 232 K (midpoint in the hysteresis loop), are identical, while an intermediate temperature phase with a different structure exists between them. Reentrant phase transitions have been often observed in liquid crystals,[11] but it is unusual in solid-to-solid phase transitions. Recently, reentrant behavior has been reported in the Cu(DCNQI) system.[12] The broken line in Figure 2a shows the best fit of the same model to the data in the intermediate temperature phase, which is obtained with $J/k_B = 108$ K and the other parameters fixed as previously. The magnetic behavior in the intermediate temperature phase can be explained in terms of a *ca.* 10% decrease of J.

DSC measurements were carried out above *ca.* 200 K, the lowest temperature attainable for reliable measurements in our apparatus and revealed an endothermic transition at 240.0 K on heating which corresponds to the higher-temperature transition. The enthalpy and entropy changes are observed to be $\Delta H = 637.5$ J mol^{-1} and $\Delta S = 2.623$ J K^{-1} mol^{-1} (or $= R$ ln 1.37), respectively.

Experimental Section

TBA[Fe(tdas)$_2$] was prepared in the general method described previously.[2] Anal. Calcd: C, 40.40; H, 6.10; N, 11.79. Found: C, 40.10; H, 5.93; N, 11.51.

(11) Cladis, P. E. *Phys. Rev. Lett.* **1975**, *35*, 48.
(12) Aonuma, S.; Sawa, H.; Kato, R.; Kobayashi, H. *Chem. Lett.* **1993**, 513 and references cited therein.

Table 1. Crystallographic Data

$FeS_6N_5C_{20}H_{36}$	$V = 1424.5(3)$ Å^3
fw = 594.74	$Z = 2$
space group = $P\bar{1}$	$\varrho_{calc} = 1.387$ g/cm^3
$a = 11.157(1)$ Å	$T = 23$ °C
$b = 13.755(2)$ Å	radiation = Mo Kα ($\lambda = 0.710\,69$ Å)
$c = 10.454(1)$ Å	$\mu = 9.69$ cm^{-1}
$\alpha = 100.93(1)°$	$R^a = 0.059$
$\beta = 107.368(9)°$	$R_w{}^b = 0.076$
$\gamma = 104.07(1)°$	

$^a R = \sum||F_o| - |F_c||/\sum|F_o|$. $^b R_w = \sum w(|F_o| - |F_c|)^2/\sum wF_o^2$.

Table 2. Fractional Coordinates and Isotropic Thermal Parameters for [Fe(tdas)$_2$]$^-$

atom	x	y	z	B_{iso},^{a} Å^2
Fe	0.47646(7)	0.37598(5)	0.97557(6)	3.66(2)
S(1)	0.3571(2)	0.2347(1)	1.0109(1)	5.24(5)
S(2)	0.3520(1)	0.3234(1)	0.7473(1)	4.43(4)
S(3)	0.6347(1)	0.3824(1)	1.1701(1)	4.93(4)
S(4)	0.6205(1)	0.4962(1)	0.9245(1)	3.99(4)
S(5)	0.0151(2)	0.0864(1)	0.6741(2)	6.92(6)
S(6)	0.9878(2)	0.5949(2)	1.2320(2)	7.12(7)
N(1)	0.1137(5)	0.1079(4)	0.8362(5)	5.8(2)
N(2)	0.1103(5)	0.1749(4)	0.6302(4)	5.6(2)
N(3)	0.8903(5)	0.5072(4)	1.2747(5)	6.1(2)
N(4)	0.8808(5)	0.5937(4)	1.0826(5)	5.7(2)
C(1)	0.2203(5)	0.1832(4)	0.8575(5)	4.5(2)
C(2)	0.2197(5)	0.2230(4)	0.7397(5)	4.2(2)
C(3)	0.7719(5)	0.4764(4)	1.1754(5)	4.6(2)
C(4)	0.7683(5)	0.5261(4)	1.0661(5)	4.3(2)

$^a B_{iso}$ is the mean of the principal axes of the thermal ellipsoid.

Table 3. Bond Distances (Å) and Angles (deg) for [Fe(tdas)$_2$]$^-$

		Distances	
Fe−S(1)	2.235(2)	S(5)−N(2)	1.642(5)
Fe−S(2)	2.242(1)	S(6)−N(3)	1.642(5)
Fe−S(3)	2.230(2)	S(6)−N(4)	1.654(5)
Fe−S(4)	2.271(2)	N(1)−C(1)	1.645(5)
S(1)−C(1)	1.728(5)	N(2)−C(2)	1.642(5)
S(2)−C(2)	1.729(5)	N(3)−C(3)	1.642(5)
S(3)−C(3)	1.726(6)	N(4)−C(4)	1.654(7)
S(4)−C(4)	1.750(5)	C(1)−C(2)	1.438(7)
S(5)−N(1)	1.645(5)	C(3)−C(4)	1.435(7)
		Angles	
S(1)−Fe−S(2)	91.61(5)	S(6)−N(3)−C(3)	106.7(4)
S(1)−Fe−S(3)	84.83(6)	S(6)−N(4)−C(4)	105.7(4)
S(1)−Fe−S(4)	167.68(6)	S(1)−C(1)−N(1)	125.4(4)
S(2)−Fe−S(3)	157.22(7)	S(1)−C(1)−C(2)	119.9(4)
S(2)−Fe−S(4)	86.78(5)	N(1)−C(1)−C(2)	114.8(5)
S(3)−Fe−S(4)	91.93(6)	S(2)−C(2)−N(2)	125.4(4)
Fe−S(1)−C(1)	102.8(2)	S(2)−C(2)−C(1)	121.8(4)
Fe−S(2)−C(2)	101.8(2)	N(2)−C(2)−C(1)	112.8(5)
Fe−S(3)−C(3)	103.3(2)	S(3)−C(3)−N(3)	124.7(4)
Fe−S(4)−C(4)	102.3(2)	S(3)−C(3)−C(4)	122.0(4)
N(1)−S(5)−N(2)	98.6(2)	N(3)−C(3)−C(4)	113.2(5)
N(3)−S(6)−N(4)	99.3(2)	S(4)−C(4)−N(4)	124.4(4)
S(5)−N(1)−C(1)	106.5(4)	S(4)−C(4)−C(3)	120.4(4)
S(5)−N(2)−C(2)	107.3(4)	N(4)−C(4)−C(3)	115.2(5)
		Intermolecular, Interatomic Distances	
Fe···Fe	3.238(1)	Fe···S(4)	2.501(2)

X-ray diffraction data were collected on a RIGAKU AFC5R automatic four-circle diffractometer with graphite monochromatized Mo Kα radiation at room temperature. Unit cell dimensions were obtained by a least-squares refinement using 25 reflections with $39.1° < 2\theta < 39.9°$. The crystal structure was solved by direct methods, and the positions of hydrogen atoms were obtained by subsequent difference Fourier syntheses or by calculations. A full-matrix least-squares technique was employed for the structure refinement in which positions of non-hydrogen atoms were treated with anisotropic thermal parameters and those of hydrogens were done with isotropic parameters. Crystal data are shown in Table 1. Atomic coordinates with isotropic thermal parameters and bond distances and angles for the [Fe(tdas)$_2$]$^-$ ion are shown in Tables 2 and 3, respectively.

Static magnetic susceptibility was measured with a Faraday balance whose details were described previously.[13]

DSC measurements were carried out on a Shimazu DSC-50 differential scanning calorimeter.

Acknowledgment. K.A. is thankful for the support by Grants-in-aid for Scientific Research Nos. 05453051 and 228/04242103 from the Ministry of Education, Science, and Culture, Japanese Government and also that from NEDO. A.E.U. acknowledges support from the SERC and the British Council.

(13) Awaga, K.; Maruyama, Y. *Chem. Mater.* **1990**, *2*, 535.

Supplementary Material Available: Listings of crystal data, atomic coordinates, anisotropic thermal parameters of non-hydrogen atoms, and bond lengths and angles (4 pages). Ordering information is given on any current masthead page.